**Supplementary Information**

# FGF21 regulates circadian behavior and metabolism by acting on the nervous system

Angie L. Bookout[1,2], Marleen H. M. de Groot[3,4], Bryn M. Owen[1], Syann Lee[2], Laurent Gautron[2], Heather L. Lawrence[1], Xunshan Ding[4], Joel K. Elmquist[2], Joseph S. Takahashi[3,4], David J. Mangelsdorf[1,4]*, and Steven A. Kliewer[1,5]*

[1]Department of Pharmacology; [2]Department of Internal Medicine, Division of Hypothalamic Research; [3]Department of Neuroscience; [4]Howard Hughes Medical Institute; [5]Department of Molecular Biology, University of Texas Southwestern Medical Center, Dallas TX 75390, USA

*To whom correspondence should be addressed. Email: davo.mango@utsouthwestern.edu; steven.kliewer@utsouthwestern.edu

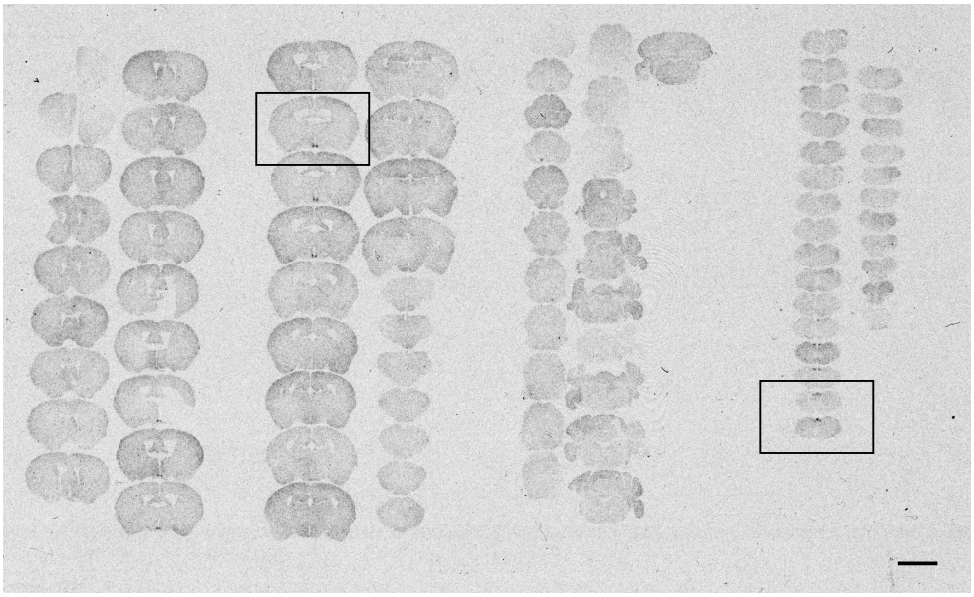

**Supplementary Figure 1** β-Klotho in situ hybridization across the mouse brain. Mouse brain coronal sections (25 μm, 1:4 series) were subjected to free-floating in situ hybridization with a $^{33}$P-labeled antisense riboprobe for *Klb* and mounted onto slides in rostral (top left) to caudal (bottom right) order. Boxed areas indicate regions shown in **Figure 1**. Bar = 45 mm.

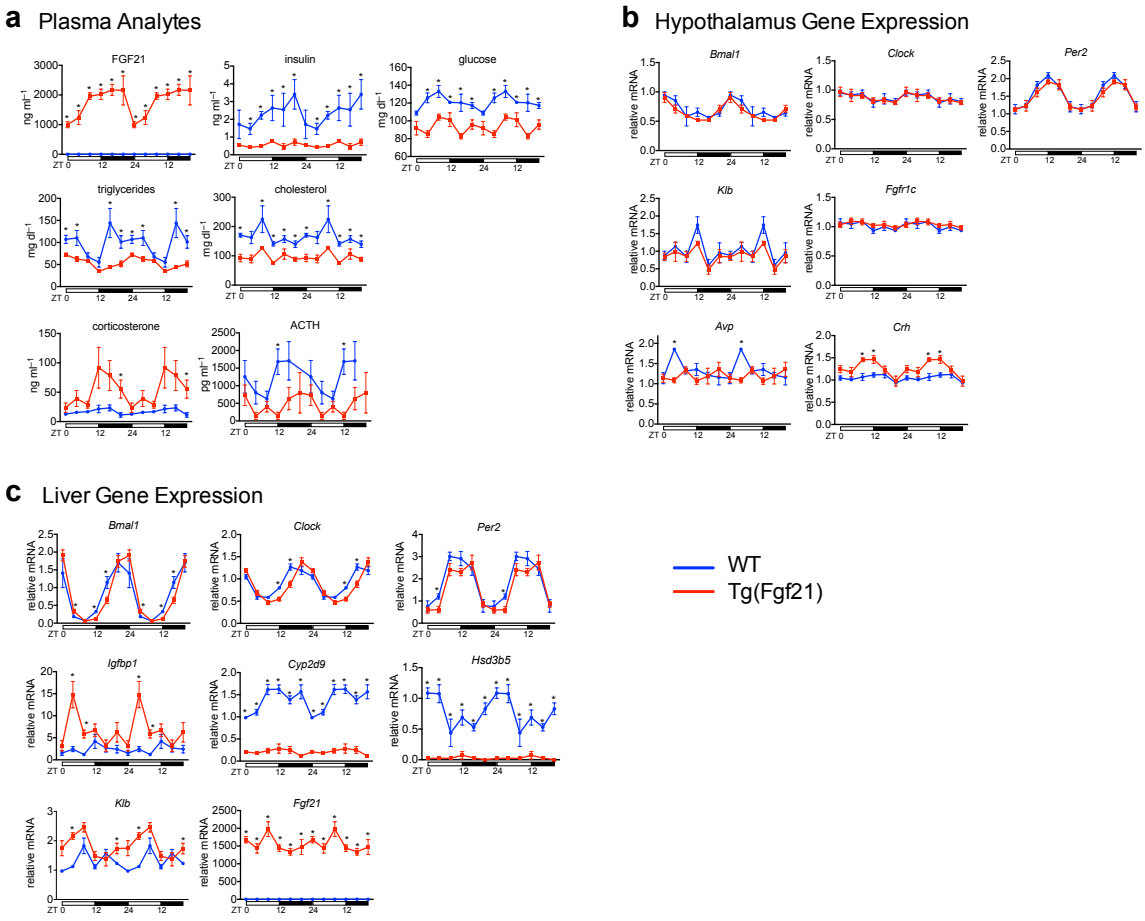


**Supplementary Figure 2** Circadian profiles of gene expression and plasma analytes in Tg(Fgf21) mice. Male wild-type (WT) or Tg(FGF21) mice were sacrificed every 4 h over a 24 h period, beginning at the start of the light phase (ZT0). (**a**) Plasma hormones and metabolites. (**b**) Hypothalamic clock, FGF21 receptor, and neuropeptide gene expression. Arginine vasopressin (*Avp*); Corticotropin releasing hormone (*Crh*). (**c**) Liver clock, growth hormone pathway, and FGF21 signaling pathway gene expression. Values on the x-axes are double-plotted; data represent mean ± SEM, $n = 3–6$. Asterisks indicate significant differences ($P < 0.05$) between WT and Tg(Fgf21).

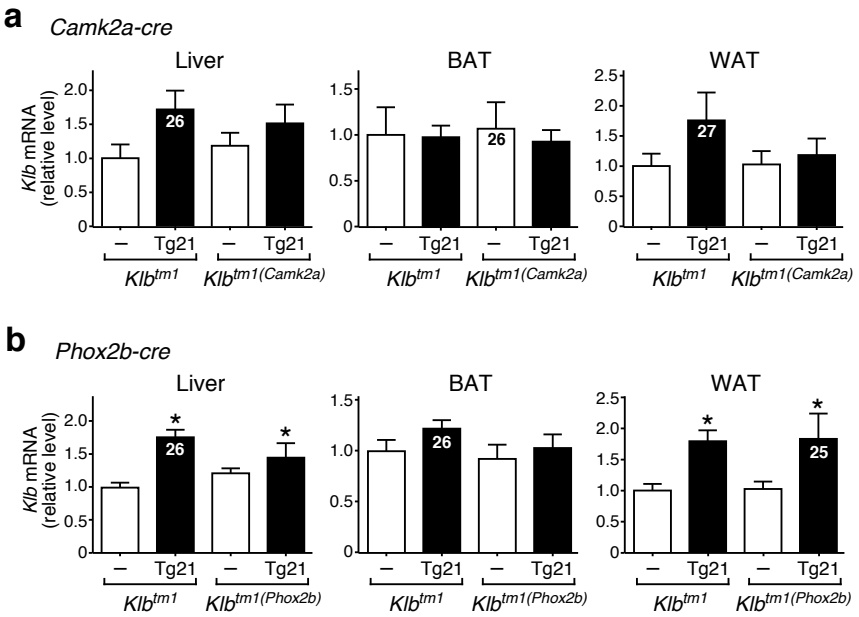


**Supplementary Figure 3** *Klb* expression is intact in peripheral tissues of the *Klb* brain knockout models. Male mice of indicated genotypes without (–) or with (Tg21) the Tg(Fgf21) insertion were sacrificed ZT8. *Klb* mRNA was quantified in liver and brown and white adipose of (**a**) *Camk2a*-cre and (**b**) *Phox2b*-cre models. Data represent mean ± SEM, $n = 5–9$. Ct values shown inside bars. Asterisks indicate significant differences ($P < 0.05$) between Tg21 and (–) control mice.

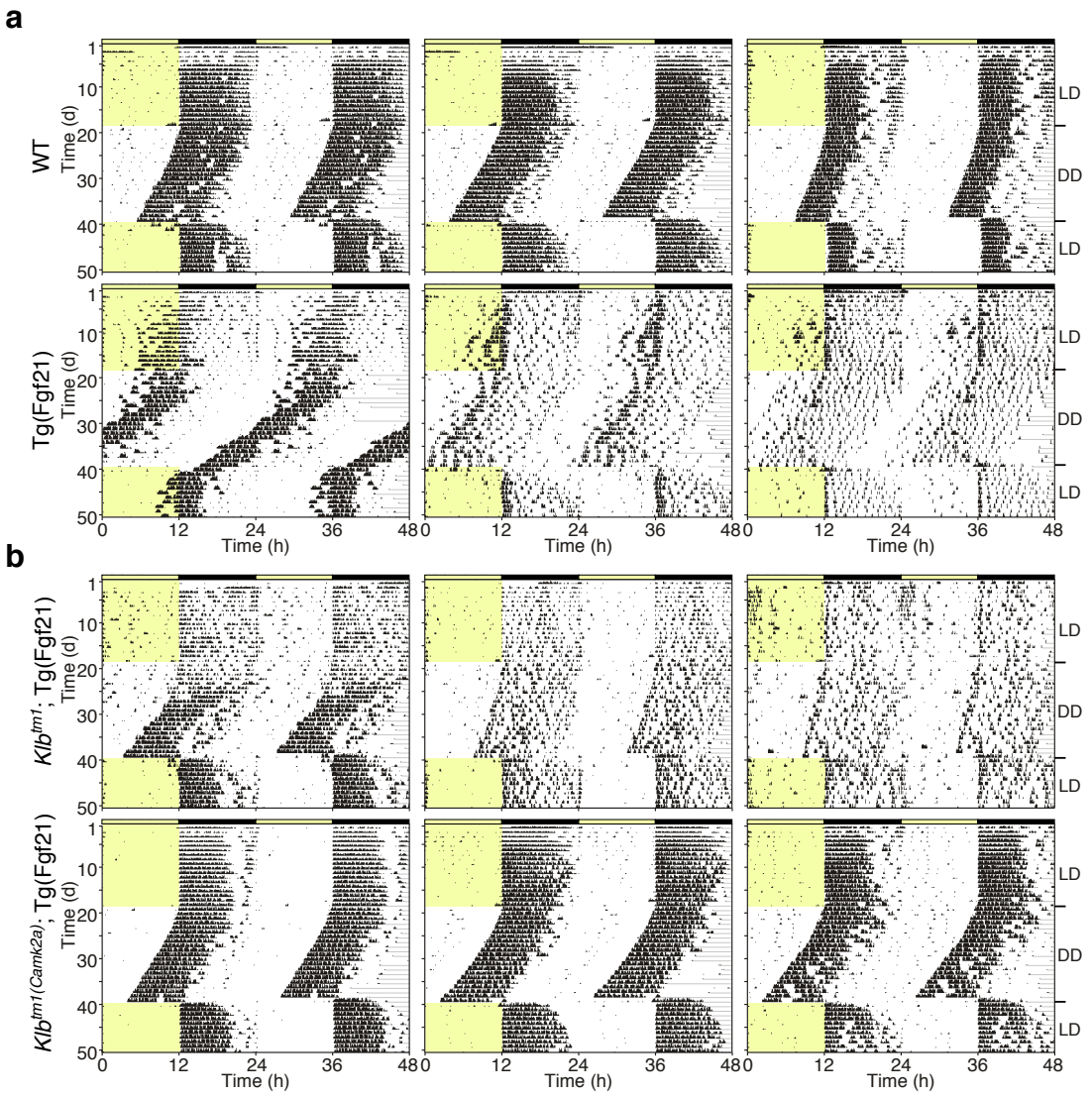


**Supplementary Figure 4** Representative actograms for Tg(Fgf21) mice. Representative actograms are shown double-plotted for three individual (**a**) wild-type (WT) or Tg(Fgf21) male mice, and (**b**) *Klb*$^{tm1}$::Tg(Fgf21) or *Klb*$^{tm1(Camk2a)}$::Tg(Fgf21) male mice (bottom). Time on x-axis refers to zeitgeber time (ZT) 0 at lights on. Yellow indicates light phase (LD, 12 hours light/12 hours dark; DD, constant darkness).

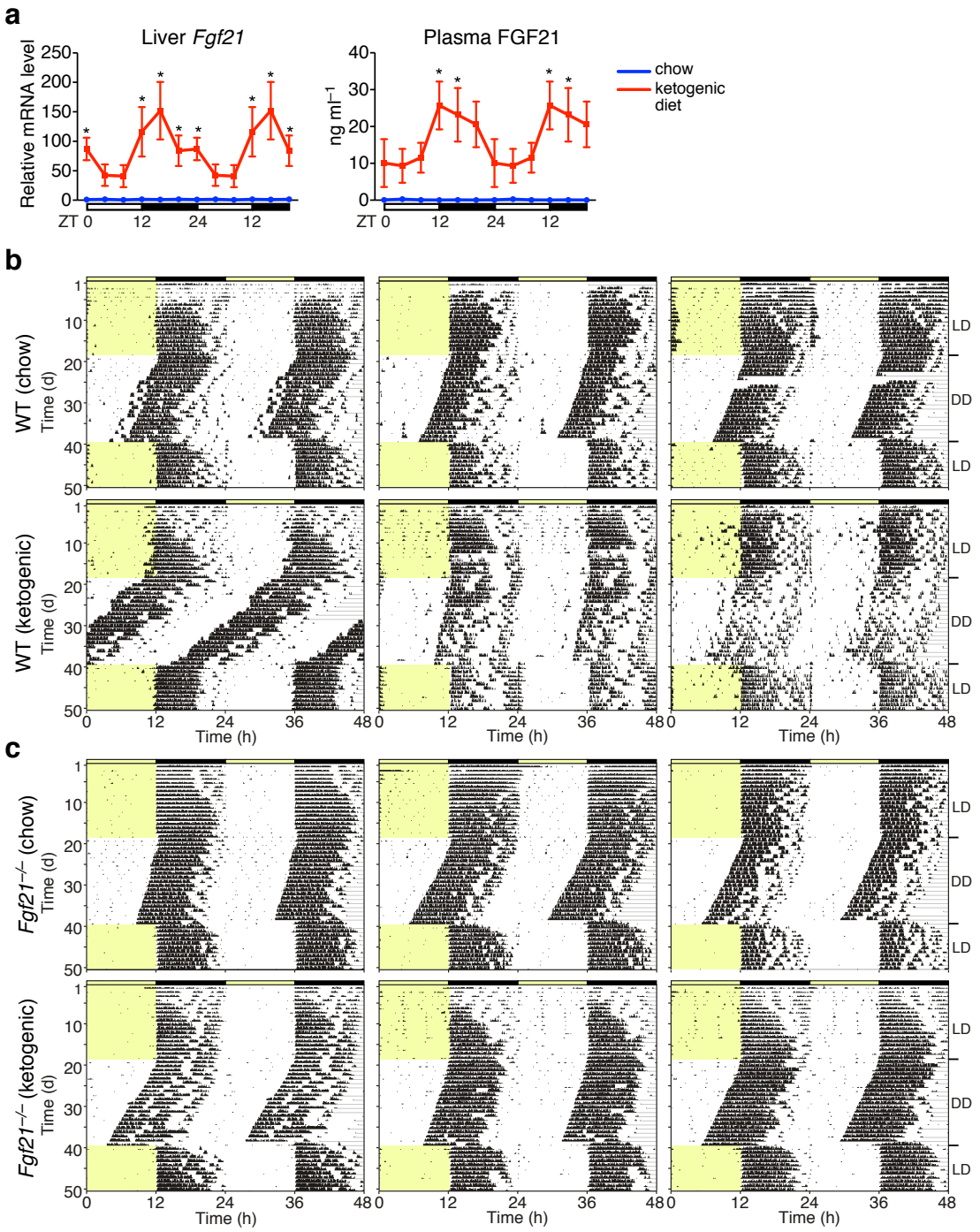


**Supplementary Figure 5** Ketogenic diet mimics transgenic FGF21 overexpression in regulating circadian behavior. (**a**) Hepatic FGF21 mRNA and plasma protein levels in male wild-type mice fed chow or ketogenic diet for 6 weeks. Mice were sacrificed every

4 h over a 24 h period, beginning at the start of the light phase (ZT0). Values on the x-axes are double-plotted; data represent mean ± SEM, $n = 4$. Asterisks indicate significant differences ($P < 0.05$) between diets. (**b, c**) Representative actograms are shown double-plotted for three individual wild-type males (**b**) fed standard chow or ketogenic diet, and *Fgf21*$^{-/-}$ males (**c**) fed standard chow or ketogenic diet. Time on x-axis refers to zeitgeber time (ZT) 0 at lights on. Yellow indicates light phase (LD, 12 hours light/12 hours dark; DD, constant darkness).

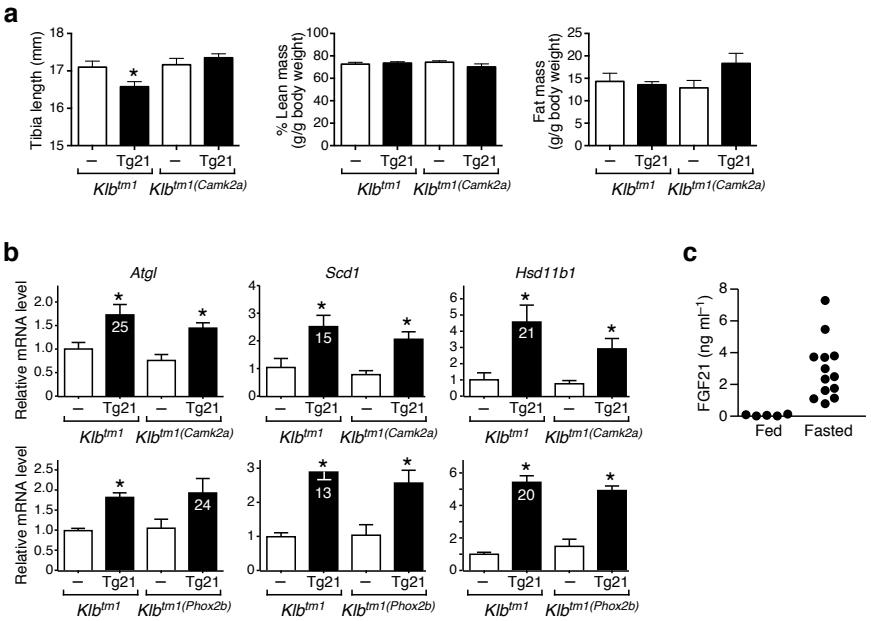


**Supplementary Figure 6** Brain-specific effects of FGF21 on growth morphometry and adipose gene expression. (**a**) Tibia length, lean mass, and fat mass from male mice of indicated genotypes without (–) or with (Tg21) the Tg(Fgf21) insertion ($n$ = 4–7). Animals were sacrificed at ZT8. (**b**) White adipose tissue gene expression in brain deletion of *Klb*. Male mice ($n$ = 5–9) of indicated genotypes were sacrificed at ZT8. Ct values shown inside bars. Data represent mean ± SEM. Asterisks indicate significant differences ($P < 0.05$) between Tg21 and (–) control mice. (**c**) Plasma FGF21 levels in individual 12-week old male C57BL/6J mice at ZT3 fed ad libitum or fasted for 24 h.

**Supplementary Table 1** Metabolic parameters from *Klb*$^{tm1(Camk2a)}$::Tg(Fgf21) and *Klb*$^{tm1(Phox2b)}$::Tg(Fgf21) mice.

| | *Klb*$^{tm1}$ | *Klb*$^{tm1}$:: Tg(Fgf21) | *Klb*$^{tm1(Camk2a)}$ | *Klb*$^{tm1(Camk2a)}$:: Tg(Fgf21) |
|---|---|---|---|---|
| *n* | 5 | 7 | 5 | 7 |
| glucose (mg dl$^{-1}$) | 130.9 ± 4.72 | 126.8 ± 4.69 | 140.8 ± 9.82 | 118.9 ± 3.86 |
| βhydroxybutyrate (μM) | 66.29 ± 8.63 | 205.4 ± 44.96* | 29.68 ± 9.65 | 45.38 ± 6.053 |
| cholesterol (mg dl$^{-1}$) | 146.1 ± 13.32 | 112 ± 6.32* | 161.1 ± 15.94 | 153.7 ± 8.67 |
| triglycerides (mg d$^{-1}$) | 50.18 ± 12.72 | 42.13 ± 5.96 | 55.9 ± 7.24 | 67.42 ± 13.74 |
| FGF21 (ng ml$^{-1}$) | 0.54 ± 0.09 | 657.4 ± 117.5* | 0.75 ± 0.15 | 737.3 ± 167.4* |

| | *Klb*$^{tml}$ | *Klb*$^{tml}$:: Tg(Fgf21) | *Klb*$^{tml(Phox2b)}$ | *Klb*$^{tml(Phox2b)}$:: Tg(Fgf21) |
|---|---|---|---|---|
| *n* | 9 | 9 | 5 | 8 |
| glucose (mg dl$^{-1}$) | 131.6 ± 3.74 | 119.3 ± 8.67 | 147.1 ± 5.19 | 112.4 ± 15.48 |
| cholesterol (mg dl$^{-1}$) | 136.6 ± 10.44 | 104.3 ± 6.20* | 128.1 ± 15.30 | 126.5 ± 5.82 |
| triglycerides (mg dl$^{-1}$) | 46.44 ± 4.08 | 49.08 ± 9.62 | 59.38 ± 6.59 | 41.33 ± 6.19 |
| FGF21 (ng m$^{-1}$) | 0.41 ± 0.70 | 784.6 ± 111.1* | 1.45 ± 0.85 | 933.5 ± 228.9* |

Data are presented as mean ± SEM. Asterisks indicate significant differences ($P < 0.05$) compared to controls without Tg(Fgf21). FGF21 measurement was taken at ZT3.

**Supplementary Table 2** Circadian wheel running parameters in *Klb*$^{tm1(Camk2a)}$::Tg(Fgf21) mice.

| | Wild-type chow | Tg(Fgf21) chow |
|---|---|---|
| *n* | 16 | 28 |
| total activity (revs/day ×$10^4$) | 2.62 ± 0.17 | 1.91 ± 0.19* |
| % light activity | 3.20 ± 0.71 | 13.94 ± 2.95* |
| % dark activity | 96.80 ± 0.71 | 86.06 ± 2.95* |
| period (h) | 23.62 ± 0.03 | 23.57 ± 0.04 |
| amplitude (%) | 17.79 ± 1.49 | 12.14 ± 1.50* |
| phase (h) | 0.24 ± 0.07 | -0.96 ± 0.37* |

| | *Klb*$^{tm1}$::Tg(Fgf21) | *Klb*$^{tm1(Camk2a)}$::Tg(Fgf21) |
|---|---|---|
| *n* | 11 | 12 |
| total activity (revs/day × $10^4$) | 0.97 ± 0.22 | 2.60 ± 0.16* |
| % light activity | 15.26 ± 3.72 | 1.87 ± 0.36* |
| % dark activity | 84.74 ± 3.72 | 98.13 ± 0.36* |
| period (h) | 23.58 ± 0.05 | 23.54 ± 0.02 |
| amplitude (%) | 7.82 ± 2.03 | 17.31 ± 1.29* |
| phase (h) | 0.13 ± 0.16 | 0.35 ± 0.06 |

Data are presented as mean ± SEM. Asterisks indicate significant differences ($P < 0.05$) compared to wild-type or *Klb*$^{tm1}$::Tg(Fgf21) controls.

**Supplementary Table 3** Circadian wheel running parameters and plasma FGF21 in wild-type versus *Fgf21*$^{-/-}$ mice.

| | Wild-type chow | Wild-type ketogenic | *Fgf21*$^{-/-}$ chow | *Fgf21*$^{-/-}$ ketogenic |
|---|---|---|---|---|
| *n* | 6 | 24 | 18 | 23 |
| total activity (revs/day × $10^4$) | 3.39 ± 0.18 | 1.86 ± 0.12* | 2.87 ± 0.20 | 2.14 ± 0.12* |
| % light activity | 3.48 ± 1.54 | 8.78 ± 1.47* | 1.81 ± 0.53† | 3.84 ± 0.76 |
| % dark activity | 96.52 ± 1.54 | 91.23 ± 1.47* | 98.19 ± 0.53† | 96.16 ± 0.76 |
| period (h) | 23.69 ± 0.02 | 23.62 ± 0.04 | 23.62 ± 0.03 | 23.64 ± 0.05 |
| amplitude (%) | 17.32 ± 2.37 | 15.41 ± 1.41 | 19.77 ± 1.06 | 19.43 ± 1.48 |
| phase (h) | 0.38± 0.20 | –0.53 ± 0.24 | 0.52 ± 0.06 | 0.03 ± 0.16* |
| Plasma FGF21 (ng ml$^{-1}$) | 0.44 ± 0.0 | 21.92 ± 5.45* | undetectable | undetectable |

Data are presented as mean ± SEM. Asterisks indicate significant differences ($P < 0.05$) compared to chow-fed mice. Daggers indicate significant differences ($P < 0.05$) compared to all other groups. FGF21 measurement was taken at ZT8.

**Supplementary Table 4** List of nuclei collected for expression profiling.

| Nucleus | Paxinos & Franklin Atlas[31] Level | Full Name |
|---|---|---|
| CTX | 40-41 | cortex |
| Thal AD | 39-40 | anterodorsal thalamic nucleus |
| OVLT | 27 | vascular organ of lamina terminalis |
| MnPO | 27 | median preoptic nucleus |
| SCN | 34-38 | suprachiasmatic nucleus |
| PVH | 37-41 | paraventricular hypothalamic nucleus |
| RCN | 39-40 | retrochiasmatic nucleus |
| LHA1 | 39 | lateral hypothalmic area to paraventricular hypothalamic nucleus |
| dmVMH | 42-46 | dorsomedial ventromedial hypothalamic nucleus |
| vlVMH | 42-46 | ventrolateral ventromedial hypothalamic nucleus |
| ARC | 42-46 | arcuate nucleus |
| cDMH | 47-48 | compact dorsomedial hypothalamic nucleus |
| vDMH | 47-48 | ventral dorsomedial hypothalamic nucleus |
| LHA2 | 47 | lateral hypothalamic area to dorsomedial hypothalamic nucleus plus perifornical area |
| PH | 51 | posterior hypothalamic area |
| PMV | 51-53 | premammillary nucleus, ventral part |
| VTA | 61 | caudal ventral tegmental area |
| mPBN | 74-75 | medial parabrachial nucleus |
| lPBN | 74-75 | lateral parabrachial nucleus |
| AP | 92-93 | area postrema |
| DMV (X) | 92-93 | dorsal motor nucleus of the vagus (Xth cranial nerve) |
| NTS | 92-93 | nucleus tractus solitarius |
| nodose | | left nodose ganglion; cell body of vagal sensory neurons |
| DRG | | mid-lower thoracic dorsal root ganglia (T7-T12) |